

Wang QINGJUN  
Hanxin CHEN  
Xubing CHEN  
Hong YANG  
Gaoping WANG

## WCZESNE WYKRYWANIE USZKODZEŃ PRZEKŁADNI ZĘBATEJ Z WYKORZYSTANIEM SŁABYCH SYGNAŁÓW DRGAŃ

### EARLY FAULT DETECTION OF GEARBOX USING WEAK VIBRATION SIGNALS

*Zaproponowano nową metodę wczesnego wykrywania pęknięć zębów przekładni zębatej polegającą na analizie słabego sygnału drganiowego zmodulowanego niskimi częstotliwościami. Uzyskaną obwiednię zmodulowanego sygnału drgań wykorzystano do wyznaczenia częstotliwości modulujących. Zdemodulowane częstotliwości charakterystyczne otrzymano za pomocą adaptacyjnej, czasowo-częstotliwościowej reprezentacji sygnału z obwiedni sygnału drganiowego wyznaczonej z wykorzystaniem transformaty Hilberta. Spektrogram adaptacyjny odzwierciedla częstotliwość zazębienia i jej harmoniczne, częstotliwość sprzęgła, częstotliwość nośną oraz wstęgi boczne w sygnale drganiowym poddanym analizie z użyciem zoptymalizowanego przekształcenia falkowego. Proponowaną metodę weryfikowano przy użyciu sygnału symulowanego i rzeczywistego. Wyniki wskazują na możliwość efektywnego zastosowania proponowanej metody do detekcji pęknięć zębów przekładni zębatej.*

**Słowa kluczowe:** wczesne wykrywanie uszkodzeń, adaptacyjna reprezentacja czasowo-częstotliwościowa, słaby zdemodulowany sygnał drań.

*A new method for the early detection of the gear crack was proposed by the analysis of the weak low-frequency modulated vibration signal. The envelope of the modulated vibration signal was extracted and used to demonstrate the modulating frequencies. The demodulated characteristic frequencies were obtained with the adaptive joint time-frequency signal representation from the Hilbert transform envelope of the vibration signal. The adaptive spectrogram matches the meshing frequency and its harmonics, the coupling frequency, the carrier frequency and the sidebands in the vibration signal by the optimized wavelet. Simulated and experimental vibration signals are used to test the proposed method. The results show the applicability and effectiveness of the proposed method for gear crack detection.*

**Keywords:** Early Fault detection, adaptive joint time-frequency, weak demodulated vibration signal.

#### 1. Introduction

The analysis of vibration signals from the gearbox casing is the most modern technique for fault detection of gearbox. The presence and type of fault at its early stage and its evolution are detected in order to estimate the machine's residual life and choose an adequate plan of maintenance [10]. The most important components in gear vibration spectra are the tooth-meshing frequency and its harmonics, together with sidebands due to the modulation phenomenon. The fault condition may change the number and the amplitude of the sidebands. The sidebands are the frequency components equally spaced around a center frequency. The center frequency called the carrier frequency is the gear mesh frequency. The faults localized on one tooth or a few teeth such as cracks and spalls produce modulation effects during the engagement of the fault teeth. Consequently, a large number of sidebands around the tooth-meshing frequency and its harmonics in the spectrum are generated and spread over a wide range, which is spaced by the rotation frequency of the faulty gear and characterized by low amplitudes [13]. Amplitude modulation can be considered to be a feature of gear crack. Ma and Li [5] developed a model-based demodulation scheme to extract the information contained in wideband gear vibration signals and reported a wideband demodulation algorithm. Lin

and Zuo [2] used an adaptive wavelet filter (by varying the parameters of the mother wavelet) to get the impulsive vibration signal for gearbox crack detection. Dalpiaz et al [7] studied the effectiveness and sensitivity of signal processing techniques for gear fault detection, including power cepstrum, time-synchronous average, and wavelet analysis.

Wavelet transform is most often used because of the feature of time-frequency localization that is capable of exhibiting the instantaneous frequencies of vibration signal and gives a description of how energy distribution over a range of frequencies from one instance to another [3, 4, 6, 9, 12]. Hilbert transform is an effective method to demodulate the vibration signal in fault diagnosis of gear [8]. It is difficult for wavelet transform and Hilbert transform to represent the characteristic frequencies from many frequency components of the faulty gear with visual inspection. The adaptive time-frequency method makes the interference coincide with the main signal components to detect the weak signals in the presence of noise, which prevents over complication of the time-frequency plane, and which also causes reinforcement of the pertinent signal features. This research proposes a new method based on the Hilbert transform and adaptive Gaussian wavelet for the demodulation of the gear vibration signal. The adaptive spectrogram is applied to analyze the vibration signal in a fine resolution. The result shows good

performance of this adaptive wavelet and great capability to detect the gear fault.

## 2. Adaptive wavelet analysis

The Gaussian wavelet is a popular non-orthogonal complex wavelet. The normalized adaptive Gaussian wavelet function is defined as:

$$\psi_p(t) = (\pi\sigma_p^2)^{-0.25} \exp\left[-(t-t_p)^2/2\sigma_p^2\right] \exp(j2\pi f_p t) \quad (1)$$

where  $\sigma_p, t_p, f_p \in R^+$ ,  $\sigma_p$  is the adjustable standard deviation and determines the tradeoff between the time and frequency resolution and  $(t_p, f_p)$  is the time-frequency center. The adaptive wavelet function  $\psi_p(t)$  can be optimally determined in the joint time-frequency domain. The ratio of the center frequency to the frequency bandwidth is  $\sqrt{2\pi\sigma_p f_p}$ , which is variable. Adaptive Gaussian wavelet function can adjust its parameter to represent the signal in fine resolution. A novel joint time-frequency algorithm based on adaptive Gaussian wavelet is adopted for adaptive signal representation [1]. This method is to use the adaptive normalized Gaussian functions to expand signal  $\phi(t)$  defined as follow:

$$\phi(t) = \sum_{p=1}^{\infty} B_p (\pi\sigma_p^2)^{-0.25} \exp\left[-(t-t_p)^2/2\sigma_p^2\right] \exp(j2\pi f_p t) \quad (2)$$

The adaptive Gaussian basis representation can match a signal by adjusting the time and frequency resolution and its time-frequency center that is different from the Gabor expansion and the wavelet decomposition. To characterize the time-varying nature of the signal, the elementary function  $\psi_p(t)$  is localized in the joint time-frequency domain and the coefficient  $B_p$  reflects the signal local behavior. Here the parameters  $\sigma_p, t_p$  and  $f_p$  are chosen such that  $\psi_p(t)$  is most similar to  $\phi(t)$ . The parameter  $\sigma_p$  can be used to adjust the bandwidth of  $\psi_p(t)$  to best match a variety of signals. The adaptive spectrogram (ADS) is obtained as follows:

$$\phi_p(t) = \phi_{p-1}(t) - B_{p-1} \psi_{p-1}(t) \quad (3)$$

$$ADS(t, f) = 2 \sum_{p=0}^{\infty} |B_p|^2 \exp\left\{-\frac{(t-t_p)^2}{\sigma_p^2} - (2\pi)^2 \sigma_p^2 (f-f_p)^2\right\} \quad (4)$$

where  $\sigma_p \in R^+, t_p \in R^+, f_p \in [0, +\infty]$ . It is shown that the exponential term in equation (4) is the WVD for a normalized Gaussian function. The adaptive spectrogram equation can be expressed as:

$$\|ADS(t, f)\|^2 = \sum_{p=0}^{\infty} |B_p|^2 = \|\phi(t)\|^2 \quad (5)$$

Equation (5) shows that the energy contained in  $ADS(t, f)$  is identical to the energy contained in the signal  $\phi(t)$ . The ADS can be considered as a signal energy distribution in the joint time-frequency domain. This adaptive spectrogram is non-negative, cross-term interference free and high in resolution. The procedure that is applied to obtaining the adaptive spectrogram is as follows: Set  $p = 1$ , where  $p$  is the index of iteration to extract the optimal parameters in equation (2) from the  $p^{th}$  signal  $\phi_p(t)$ .

- (1) Obtaining the optimal parameters  $(B_p, f_p, t_p, \sigma_p)$  by minimizing  $E_p$  the following section as shown in the following equation

$$E_p = \sum_{i=1}^K |\phi_p(t_i) - B_p \psi_p(t_i)|^2 \quad (6)$$

- (2) As shown in equation (3), obtain the remaining signal  $\phi_{p+1}$  after subtracting the signal obtained in step 2.
- (3) Let  $p = p+1$ . Return to step 2 unless the reconstructed error  $E_p$  is sufficiently small.
- (4) The optimal parameters are then applied to equation (4) to obtain the adaptive spectrogram.

The algorithm is coded in Matlab by the authors. Genetic algorithm (GA) is used to optimize the parameters in equation (2). For details on GA, check ref. [11]. The chromosome (C) contains the five real numbers of the features. The features represent the four parameters of the model as shown in equation (2). An example is shown as:

$$C = \{c_1, c_2, c_3, c_4, c_5\} = \{real(B_p), imag(B_p), f_p, t_p, \sigma_p\} = \{0.003, -0.002, 55, 0.04, 0.003\} \quad (7)$$

The numbers in the chromosome represent respectively the real part and the imaginary part of the amplitude, the center of the frequency, the time and the standard deviation. The objective function is the sum of squared error function in equation (6). The GA procedure is applied to obtain the next optimal parameters again. So the results of all the optimal parameters applied in equation (2) are the optimal signal representation of the original signal  $\phi(t)$ . The optimal parameters are also used in equation (4) to obtain the adaptive spectrum.

## 3. Gearbox Experimental System

The experimental vibration signals collected from a gearbox dynamics simulator of SpectraQuest are employed to test the proposed method. Two accelerometers of model PCB 352C67 are mounted on the gearbox in both vertical and horizontal directions. Through the signal conditions, the vibration data is acquired by DSP Siglab 20-42 Signal Analyzer and Dell Inspiration 7500 laptop. The transmission diagram of the gearbox is shown in Figure 1. Five spur gears are installed on three shafts. The vibration generated by the impact force between gears 3 and 4 is in the vertical direction as shown in Figure 1. The vertical sensor can catch the vibration signal with higher sensitivity along the vertical direction. Gear 3 is chosen to be the one to be studied in this experiment. Figure 2 shows the gear crack on this gear in the experiment. The crack occurs along the normal line of the tooth's root curve. The angle of the crack with the line  $a$  is in the range of  $40^\circ$ - $50^\circ$ . The crack angle in the faulty gear 3 is  $45^\circ$ . The sampling frequency is  $2.56 \times 1k$  ( $1k=1024$ ). The number of data points in each sample is set at 2048. The rotational speed of the motor is 800 rpm. The load force by the brake is half of 51.77 Nm. Based on the drive ratios between the teeth number of teeth of the driving gear and the teeth number of teeth of the driven gear, and rotational speed of the drive motor, the rotational speed and the characteristic frequency of each gear are determined as shown in Table 1. Here  $F_1$  is the rotational speed of shaft 1 and gear 1,  $F_2$  is the rotational speed of shaft 2 and gears 2 and 3,  $F_3$  is the rotational speed of shaft 3 and 4,  $F_{12}$  is the meshing frequency of gears 1 and 2 and  $F_{34}$  is the meshing frequency of gears 3 and 4.

Tab.1. Rotational speeds and characteristic frequencies of the gears

Motor(rpm)	Torque (Nm)	F <sub>1</sub> (Hz)	F <sub>12</sub> (Hz)	F <sub>2</sub> (Hz)	F <sub>34</sub> (Hz)	F <sub>3</sub> (Hz)
800.0	51.77/2	3.17	152.38	9.52	228.57	5.71

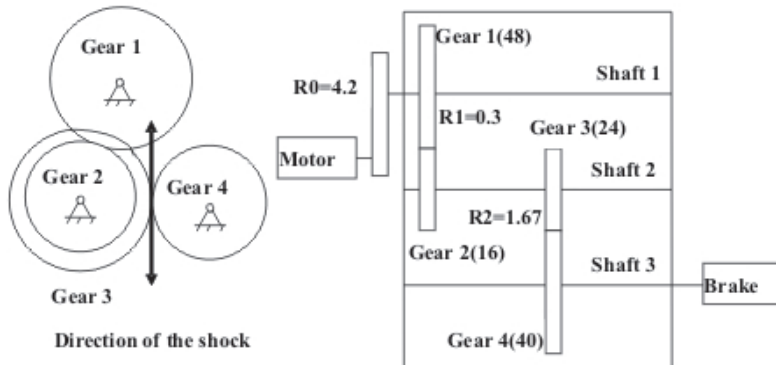


Fig. 1. The diagram of the experimental system

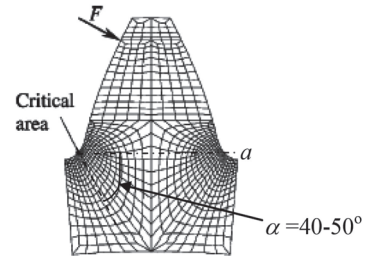


Fig. 2. The sectional area of gear tooth

4. Results and discussion

A simulated signal is used to test the proposed method in Equation 8. The signal  $\cos(2\pi \cdot 1560t) + \cos(2\pi \cdot 1600t)$  in time interval  $[0, 0.5]$  is modulated by frequencies of 40 Hz and 80 Hz. The 80 Hz frequency exists during the time period of  $(0, 0.099)$  and  $(0.301, 0.5)$  seconds, which simulates that the modulating frequency varies with time. Both amplitude and phase modulations are considered in the simulated signal. The frequency component  $(1560+40)$  Hz is set to equal to one of the original signal frequency of 1600 Hz. Here  $Rand(t)$  denotes the normally distributed white noise.

$$x(t) = 0.7(1 + \sin(80\pi t)) \cos(3120\pi t + \sin(80\pi t)) + 1.5Rand(t)$$

$$+ \begin{cases} (1 + \sin(160\pi t)) \times \\ \cos(3200\pi t + \cos(3200\pi t + \cos(3200\pi t + \sin(160\pi t)))) \\ t = [0, 0.099] \\ \cos(3200\pi t) \quad t = [0.1, 0.3] \\ (1 + \sin(160\pi t)) \cos(3200\pi t + \sin(160\pi t)) \\ t = [0.301, 0.5] \end{cases} \quad (8)$$

The sampling frequency of the simulated signal is 4 kHz (1k=1024). The proposed method is applied to analyze the simulated signal to get the modulated signal of 40 Hz and 80 Hz frequency components. Firstly, Hilbert transform is used to analyze the simulated signal to generate the signal envelope. Figure 3(a) shows the spectrum of the simulated signal defined in equation (8). There are some sidebands around the frequency of 1600 Hz, which are 1520 Hz, 1560 Hz and 1680 Hz. It is not clear that there is a modulated signal with 40 Hz and 80 Hz frequency components in it. Secondly, Hilbert transform is used to analyze the simulated signal in figure 3(a). Figure 3(b) shows the power spectrum of the Hilbert transform signal envelope. The signal envelope of the Hilbert transform includes the 40 Hz and 80 Hz signal components. It does not differentiate the carrier frequencies of 1560 Hz and 1600 Hz, modulating frequencies of 40 Hz and 80 Hz and the coupled frequencies.

In order to demodulate the 40 Hz and 80 Hz frequency components from the signal envelope by Hilbert transform, the proposed adaptive spectrogram is used to analyze the signal envelope of Hilbert transform. Figure 4 shows the adaptive spectrogram of the signal envelope from Hilbert transform as shown in figure 3(b). The 40 Hz and 80 Hz frequency components can be differentiated and identified clearly, especially the time range of the 80 Hz frequency is shown in detail, which is the same as equation (8). The proposed method based on the Hilbert transform and adaptive spectrogram is effective to demodulate the modulated frequency component of the simulated signal.

The experimental vibration signals collected from the gearbox dynamics simulator of SpectraQuest are used to test the proposed method. When a gear has a local fault such as crack, the vibration signal of the gearbox contains amplitude and phase modulations, which are periodic with the rotational frequency of the gear. The modulation of the meshing frequency from the faulty gear generates the sidebands. The sidebands are either the shaft rotational speed or one of its multiples. As described in Section 3, the gear 3 has a crack, the sidebands on the rotational speed and its harmonics are produced as the modulation from the gear.

In order to demodulate the sidebands generated by gears 3, 4 and 5 on shafts 3, gears 4 and 5, Hilbert transform is used

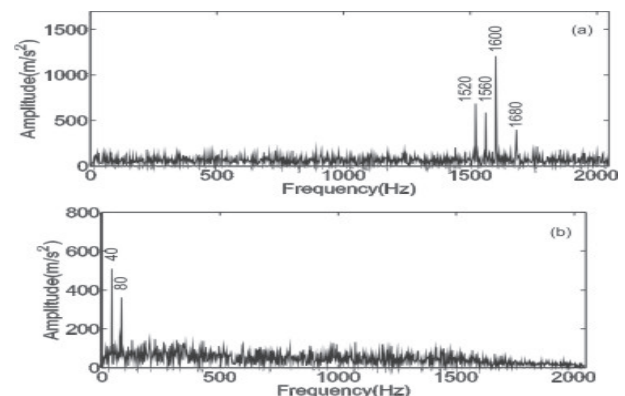


Fig. 3. (a) Spectrum of the simulated signal, (b) Spectrum of the simulated signal envelope with Hilbert transform

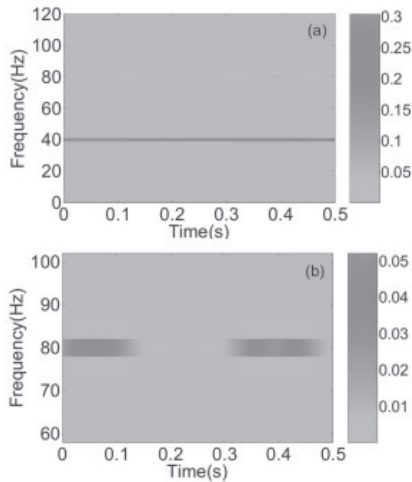


Fig. 4. The adaptive spectrogram of the simulated signal envelope from Hilbert transform (a) (0,120) Hz (b) (60,100) Hz

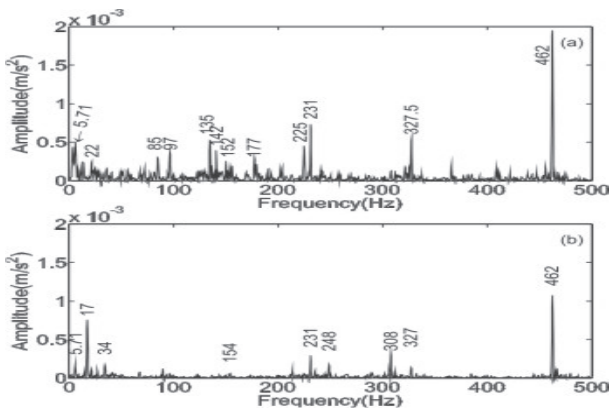


Fig. 5. Power density spectrum of the Hilbert transform envelope of the experimental vibration signals (a) the normal gearbox (b) the faulty gearbox

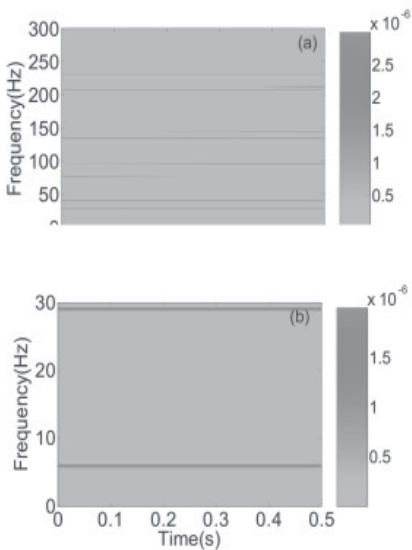


Fig. 6. The adaptive spectrogram of the experimental vibration signal envelope from Hilbert transform under normal condition (a) (0,300) Hz (b) (0,30) Hz

to analyze the experimental vibration signal. Figure 5 Power density spectrum of the Hilbert transform envelope of the experimental vibration signals under normal condition and faulty condition. Figure 5(a) shows the center frequency components of 5.17 Hz generated by gears 4. The meshing frequency components of 152 Hz and 231 Hz between gears 1, 2 and gears 3, 4 are presented. Figure 5(b) shows the center frequency components of 5.71 Hz generated by gear 4 and meshing frequency components of 154 Hz and 231 Hz generated between gears 1, 2 and 3, 4. Although the frequency components of 5.71 Hz and 231 Hz are shown in figure 5(a) and (b) at the same time and their amplitudes are different, there are harmonic frequency components around the frequencies generated by the gears 3 and 4 in figure 5(a) and (b). It is not enough to identify the fault gear by using the power density spectrum of the Hilbert transform envelope. We need to demodulate the frequency of 5.71 Hz by the gear 4 in the time-frequency domain.

The adaptive spectrogram is applied to analyze the Hilbert transform envelope of the vibration signal. Figure 6 shows the results by the adaptive spectrogram of the Hilbert transform under normal condition. It shows the modulating frequency of 5.71 Hz in gear 4 and meshing frequency of 228.57 Hz between gears 3, 4 clearly. Figure 7 shows the results by the adaptive spectrogram of the Hilbert transform under faulty condition. The modulating frequency of 5.71 Hz in gear 4 and meshing frequency of 228.57 Hz between gears 3, 4 are identified. The amplitudes of frequencies 5.71 Hz and 228.57 Hz are different by comparison between figures 6 and 7. As we discussed, when there is crack in gear, the rotational frequency and meshing frequency of the faulty gear are generated. The results in figures 6 and 7 show that the proposed method demodulates the frequency component of 5.71 Hz in gear 4 and meshing frequency component of 228.57 Hz effectively and clearly, which is used to detect the early gear fault in the gearbox.

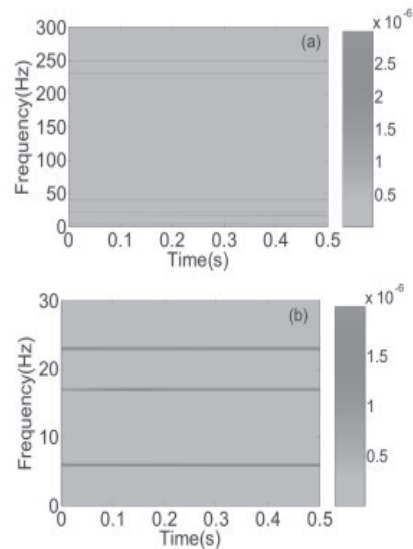


Fig. 7. The adaptive spectrogram of the experimental vibration signal envelope from Hilbert transform under faulty condition (a) (0,300) Hz (b) (0,30) Hz

#### 4. Conclusion

This paper proposed a new method based on Hilbert transform and adaptive spectrogram for the early fault detection of gearbox by demodulation of the weak modulating frequency

components and meshing frequency to detect the gear crack. Both simulated signal and experimental vibration signal are used to test the proposed method. The results show the applicability for the adaptive spectrogram to extract and identify the demodulating frequencies in fine resolution.

\*\*\*\*\*

*The experimental data is provided by the Reliability Research Lab in the Department of Mechanical Engineering at the University of Alberta in Canada. The project is supported by the Natural Science Foundation of Hubei Province of China (2008CDB300), Major project of Hubei Provincial Department of Education (Z20101501) and the Natural Sciences and Engineering Research Council of Canada (NSERC).*

\*\*\*\*\*

#### 5. References

1. Chen H. X, Chua P. S. K, Lim G. H., Vibration Analysis With Lifting Scheme and Generalized Cross Validation in Machinery Fault Diagnosis. *Journal of Sound and Vibration* 2007; 301(3-5): 458-480.
2. Chen H. X, Chua P. S. K, Lim G. H, Adaptive wavelet transform for model of vibration signal and application in fault diagnosis of water hydraulic motor. *Mechanical Systems and Signal Processing* 2006; 20(8): 2022-2045.
3. Dalpiaz G, Rivola A, Rubini R, Effectiveness and sensitiveness of vibration processing techniques for local fault detection in gears. *Mechanical Systems and Signal Processing* 2000; 4(3): 387-412.
4. Hoseini M, Mandal M. K, Zuo M. J, and Mani G, Gearbox fault diagnosis using Hilbert transform and segmented regression. *Proceedings of the Fifth International Conference on Condition Monitoring & Machinery Failure Prevention Technologies*, Edinburgh, Scotland, UK, July 14 - July 18, 2008: 650-656.
5. Li Z, Han J, Sun J, He Y, Chu F, Fault recognition method based on independent component analysis and hidden Markov model. *Journal of Vibration and Control* 2007; 13( 2): 125-137.
6. Li Z., He Z. J, Zi Y. Y. Jiang H. K, Rotating machinery fault diagnosis using signal-adapted lifting scheme. *Mechanical Systems and Signal Processing* 2008; 22(3): 542-556.
7. Lin J, Zuo M. J, Gearbox fault diagnose using adaptive wavelet filter. *Mechanical Systems and Signal Processing* 2003; 17(6): 259-1269.
8. Ma B, Ma R, Jiang Z, Gao J, A system of real-time monitoring and fault self-recovering for centrifuge. *Journal of Beijing University of Chemical Technology (Natural Science Edition)* 2005; 32(3): 92-94.
9. Ma J, Li C. J, Gear defect detection through model-based wideband demodulation of vibrations. *Mechanical System and Signal Processing* 1996; 10(5): 653-665.
10. Qian S. Chen D, Signal representation using adaptive normalized Gaussian functions. *Signal Processing* 1994; 36(1): 1-11.
11. Sun W, Chen J, Li J, Decision tree and PCA-based diagnosis of rotating machinery. *Mechanical Systems and Signal Processing* 2007; 21(3): 1300-1317.
12. Yimin Shao, Xiaoxia Li, Chris K. Mechefske and Zaigang Chen, Rear axle gear damage prediction using vibration signal preprocessing coupled with RBF neural networks, *Eksplotacja i Niezawodnosc – Maintenance and Reliability* 2009; 4(44): 57-64.
13. Yu D, Yu Y, Cheng J, Application of time-frequency entropy method based on Hilbert-Huang transform to gear fault diagnosis. *Source: Measurement: Journal of the International Measurement Confederation* 2007; 40(9-10): 823-830.

---

**Prof. Wang QINGJUN**

**Prof. Hanxin CHEN**

**Prof. Xubing CHEN**

**Prof. Hong YANG**

**Prof. Gaoping WANG**

School of Mechanical and Electrical Engineering

Wuhan Institute of Technology

693#, XiongChu Road, Wuhan, P.R. China

e-mail: pg01074075@ntu.edu.sg

---